| ORIGINAL ARTICLE OPEN ACCESS

Thermal Convection in a Sixth-Order Generalized Navier–Stokes Fluid

Giulia Giantesio[1] | Alberto Girelli[1] ⬤ | Chiara Lonati[2] | Alfredo Marzocchi[1] | Alessandro Musesti[1] | Brian Straughan[3]

[1]Dipartimento di Matematica e Fisica "N. Tartaglia," Università Cattolica del Sacro Cuore, Brescia, Italy | [2]Dipartimento di Scienze Matematiche "G.L. Lagrange," Politecnico di Torino, Torino, Italy | [3]Department of Mathematical Sciences, University of Durham, Durham, UK

Correspondence: Alberto Girelli (alberto.girelli@unicatt.it)

ABSTRACT

In this work, we deal with a problem of thermal convection for a fluid satisfying Navier–Stokes equation containing the spatial derivatives of the velocity field of sixth order, with the introduction of a tri-Laplacian term. It was pointed out by several authors, for example, Fried and Gurtin, that contributions of higher order take into account microlength effects; these phenomena are relevant in microfluidic flows. In particular, we follow the isothermal model of Musesti, using a Boussinesq approximation, so that the density in the body force term depends on the temperature to consider buoyancy effects that occur when the fluid is heated and it expands. We discuss different meaningful boundary conditions that have a key role to understand the effects of higher-order derivatives in microfluidic scenarios with convection. We carry out the complete study of linear and nonlinear stability for the flow. In addition, we complete the treatment with the analysis of critical wavenumbers and Rayleigh numbers for convection in the fluid.

1 | Introduction

In recent years, nonstandard fluids which may be called generalized Navier–Stokes fluids have gained considerable interest both from the theoretical and the experimental point of view, see, for instance [1, 2]. As an example, Navier–Stokes–Voigt fluids (see, e.g., [3–9]), which are a zero-order theory in a larger class called Kelvin–Voigt fluids, have been deeply investigated by the Russian school, also with possible thermal effects [10–17]. Besides these, also Ladyzhenskaya's alternative formulations are worth mentioning [18–21].

Among these formulations, the ones which involve higher spatial derivatives of the velocity field are of particular interest to this study. As a matter of fact, they may be helpful in the rapidly expanding theory of flow in microdevices, as well as in the area of microfluidics (cf. [22–24]). Generalized Newtonian theories of this type were studied by [22, 25, 26], while

the higher derivative theories in [27–30]. In [31], it also has been proved that these theories are fully compatible with a generalized balance law of higher gradient powers.

To be more precise, the prime aim of the present paper is to analyze a class of generalized Navier–Stokes fluids having the viscous term involving not only the Laplacian of the velocity field, but also the bi- and the tri-Laplacian of the velocity field, this theory having been developed by [28]. We notice that theories of sixth order were previously considered by Nikolaevskiy [32] in the context of viscoelasticty and Beresnev and Nikolaevskiy [33] in the modeling of nonlinear seismic waves. The Nikolaevskiy equation has been more recently studied also in [34, 35]. Interestingly, a sixth-order thin-film equation appears in the context of reduced models for fluid-structure interaction systems (see [36, 37]).

In classical viscous fluid dynamics, the Cauchy stress tensor T_{ij} depends linearly on the symmetric part of the velocity gradient,

$$d_{ij} = \frac{1}{2} \left(v_{i,j} + v_{j,i} \right),$$

where $\mathbf{v}(\mathbf{x}, t)$ denotes the velocity field at a point $\mathbf{x}$ at time t, and $v_{i,j} \equiv \partial v_i / \partial x_j$.

This theory is well-established for ordinary fluids, but for situations where the composition of the fluid may involve long molecules, or where the length scales involved are extremely small, the sixth-order theory of [28] may be very relevant. The new theory argues that the total stress tensor depends not just upon the velocity gradient, but also upon the first spatial derivative of the spatial gradient of the velocity, and also upon the second spatial derivatives of the gradient of the velocity, that is, upon $v_{i,jk} \equiv \partial^2 v_i / \partial x_j \partial x_k$ and upon $v_{i,jkh} \equiv \partial^3 v_i / \partial x_j \partial x_k \partial x_h$.

This article studies the thermal convection in the sixth-order theory including temperature effects via a Boussinesq approximation (see, e.g., [38]). We analyze thermal convection, in particular both global nonlinear stability and linear instability theory, and we find that this leads to novel behavior. Indeed, stability in thermal convection is an area where many novel effects are being found (see, e.g., [39–42]). Novel results are being achieved especially using the nonlinear energy stability method (see, e.g., [43–46]). Moreover, thermal convection in fluids is yielding very novel and important results in the field of renewable energy, as pointed out in [47].

One of the key aspects of the present work is to pay particular attention to the correct form of boundary conditions needed when higher-order derivatives are present. A set of partial differential equations is generally useless if it is not completed by correct boundary conditions which are applicable to real-life situations and which describe the interaction with the outside. Since for the model we investigate the momentum equation involves the bi- and tri-Laplacian terms $\Delta^2 v_i$, $\Delta^3 v_i$, Δ being the usual Laplace operator, finding the further boundary conditions for the problem is a difficult matter. In this regard, we appeal to the fundamental paper [27] regarding boundary conditions, although the extension to the present sixth-order theory [28] requires a new approach.

In this work, we present the model for thermal convection in a generalized sixth-order Navier–Stokes fluid, followed by its application to study Bénard convection—a phenomenon in which a layer of fluid, heated from below, exhibits convective motion. We examine the stability conditions for this problem from both a linear instability perspective and a nonlinear viewpoint using energetic methods. The boundary conditions are broken down into three main physically relevant cases and detailed numerical results are presented and interpreted.

2 | The Model for Convection With Higher-Order Spatial Derivatives

We start from [28, eq. 22] to study the convection problem, the system of equations describing the phenomena will also involve a relation for the temperature, that will be an energy balance that exploits the classical Boussinesq approximation [38]. The arising attention to phenomena occurring at small length scales justifies this generalization because terms with higher derivatives affect the behavior of the fluid at these orders. The main contribution in the literature to the description and analysis of a viscous flow in the setting of higher-order contributions is due to Fried and Gurtin [27], where second-gradient fluids and corresponding derivatives up to the fourth order are considered, with the definition of a hyperstress by a tensor of third order denoted by G; this is extended in [28] by the introduction of third gradients. They also carefully study possible boundary conditions for this kind of fluids, that are relevant because of the introduction of new terms with higher-order derivatives. This approach traces back to the work of Germain [48, 49], who first introduced higher-order derivatives in the virtual displacements in order to describe the microstructure of a body.

We proceed now to present the fundamental equations for an incompressible fluid considering also third gradients; we have the system of equations

$$\begin{cases} \frac{\partial \mathbf{v}}{\partial t} + (\mathbf{v} \cdot \nabla)\mathbf{v} = \mathbf{f} - \frac{1}{\rho}\nabla p + \nu \Delta \mathbf{v} - \hat{\xi}\Delta^2 \mathbf{v} + \hat{\gamma}\Delta^3 \mathbf{v} \\ \operatorname{div} \mathbf{v} = 0, \end{cases} \tag{1}$$

where ρ is constant being an incompressible fluid, $\mathbf{f}$ is an external body force, $p(x,t)$ is the effective pressure, Δ is the Laplacian, and ν is the positive constant kinematic viscosity of the fluid, $\hat{\xi}, \hat{\gamma}$ are the positive coefficients of [28] divided by ρ.

We will denote a general point as $\mathbf{x} = (x_1, x_2, x_3) \equiv (x, y, z)$ and the components of the velocity as $\mathbf{v} = (v_1, v_2, v_3) \equiv (u, v, w)$. For the formulas written in components, we will use Einstein convention.

To treat the coupling between velocity and temperature, we assume that ρ is linear in the temperature field, so that

$$\rho = \rho_0 \left[1 - \alpha(T - T_0)\right], \tag{2}$$

where ρ_0 is a constant, α denotes the thermal expansion coefficient of the fluid, and T_0 is a reference temperature.

The density is assumed constant everywhere else. Using the Boussinesq approximation, we obtain the system of equations

$$\begin{cases} \frac{\partial \mathbf{v}}{\partial t} + (\mathbf{v} \cdot \nabla)\mathbf{v} = -\frac{1}{\rho}\nabla p + \nu \Delta \mathbf{v} - \hat{\xi}\Delta^2 \mathbf{v} + \hat{\gamma}\Delta^3 \mathbf{v} + \alpha g T \boldsymbol{k} \\ \operatorname{div} \mathbf{v} = 0 \\ \frac{\partial T}{\partial t} + \mathbf{v}\nabla T = \kappa \Delta T, \end{cases} \tag{3}$$

where g denotes the gravity along the z-direction, with negative verse, κ represents the thermal diffusivity and $\boldsymbol{k} = (0,0,1)$.

The problem of existence of a flow satisfying the isothermal model with bi-Laplacian is studied in [30] and [29]. Interesting instability results for the isothermal model (1) have been given by [50], assuming boundary conditions periodic in space.

In this work, we will present the study of linear and nonlinear instability for the setting just presented for Bénard convection. As regards the possible boundary conditions to be assigned to the flow, we follow the approach of [27], completing them with the necessary modifications because of the presence of the tri-Laplacian, as in [28], that originates a richer structure. We will present and treat three classes of different boundary conditions, called strong adherence, weak adherence, and general adherence, inspired to the ones treated in [27] for second-gradient fluids.

3 | Stationary State, Perturbation, and Adimensionalization of the Problem

The domain of the problem is the layer $\{(x,y) \in \mathbb{R}^2\} \times \{0 < z < d\}$. Let T_L and T_U be two constants such that $T_L > T_U$. We require that it holds $v_3 = 0$ at $z = 0, d$, that the temperature is $T = T_L$ at $z = 0$ and that the temperature is $T = T_U$ at $z = d$.

The system of governing equations is satisfied by the basic state

$$\bar{v}_i \equiv 0, \qquad \bar{T} = -\beta z + T_L, \tag{4}$$

where β is the temperature gradient, namely,

$$\beta = \frac{T_L - T_U}{d}$$

and $\bar{p}$ can be determined from the momentum equation.

The stationary solution is denoted by $(\bar{v}_i, \bar{T}, \bar{p})$ and we consider its perturbation denoted by (u_i, θ, π), with

$$v_i = \bar{v}_i + u_i, \quad T = \bar{T} + \theta, \quad p = \bar{p} + \pi,$$

where $\bar{p}$ is the steady-state pressure. We adimensionalize the governing equations of the perturbation with the quantities

$$u_i = u_i^* U, \qquad x_i = x_i^* d, \qquad t = t^* \mathcal{T}, \qquad \xi = \frac{\hat{\xi}}{\nu d^2},$$

$$\theta = \theta^* T^\sharp, \qquad \pi = \pi^* \tilde{P}, \qquad P = \frac{\rho_0 \nu U}{d}, \qquad \gamma = \frac{\hat{\gamma}}{d^2 \nu},$$

$$T^\sharp = U\sqrt{\frac{\beta\nu}{\kappa\alpha g}}, \qquad Ra = R^2 = \frac{\alpha\beta g d^4}{\kappa\nu},$$

where Ra is the Rayleigh number.

We thus obtain the adimensional equations for the perturbation:

$$\begin{cases} \frac{\partial \mathbf{u}}{\partial t} + (\mathbf{u}\cdot\nabla)\mathbf{u} = -\nabla\pi + \Delta\mathbf{u} - \xi\Delta^2\mathbf{u} + \gamma\Delta^3\mathbf{u} + R\theta\boldsymbol{k} \\ \operatorname{div}\mathbf{u} = 0 \\ Pr\left(\frac{\partial\theta}{\partial t} + \mathbf{u}\nabla\theta\right) = Rw + \kappa\Delta\theta, \end{cases} \tag{5}$$

where $Pr = \nu/\kappa$ is the Prandtl number.

4 | Boundary Conditions

Although we follow the development of boundary conditions as in [27], it is necessary to incorporate the structure presented by the sixth-order theory of [28]. This leads to a different set of boundary conditions from those obtained for the four derivatives model of [27] and [28]. As stressed in [27], the importance of the boundary conditions is not only a matter of correct physical description, but also key to any stability study. The external power on a body is that generated by the tractions and velocities on the boundary together with any external body forces, while the internal power is that generated by internal stresses paired with velocity gradients. The principle of virtual power requires these to be equal on any control volume, see [27, p. 522] and a dissipation inequality is provided by the free energy imbalance. In other words, the temporal increase in free energy of an arbitrary region in the body is less than or equal to the power expended in that region, [27, p. 528]. This allowed [30] to obtain restrictions on coefficients of the power expended and essentially in our case leads to the right-hand side of (24) being nonnegative. This is very important for asymptotic stability.

The topic of boundary conditions in thermal convection has garnered significant recent interest. It is essential to take great care in selecting the form of boundary conditions to properly represent the physical problem at hand (cf. [51–57]).

The governing equations for the perturbation variables are presented in (5). The solution is supposed to be periodic in x, y and satisfies a plane tiling planform, typically having a hexagonal shape (cf. the detailed discussion in [58, pp. 43–52]). The temperature boundary conditions are as usual

$$\theta = 0 \qquad \text{on} \quad z = 0, 1. \tag{6}$$

Much more care has to be taken with the boundary conditions for the velocity perturbation u_i. We denote by V a convection cell, which is typically hexagonal, and the boundary intersecting with $z = 0$ will be denoted by Γ_1, while the boundary intersecting with $z = d$ by Γ_2.

The discussion below applies to boundary conditions for the perturbation velocity. Since the boundary conditions for the sixth-order case were not derived by [28], we first derive the correct boundary conditions for a general three-dimensional domain Ω having Γ as boundary, and the general boundary conditions are specialized to the thermal convection problem between two planes afterward.

Equation (5) has, in general, the form

$$u_{i,t} + u_j u_{i,j} = \sigma_{ij,j} + R\theta k_i, \tag{7}$$

where σ_{ij} is the total stress tensor. This tensor is composed of three parts. There is the symmetric Cauchy stress, T_{ij}, which has the classical expression

$$T_{ij} = -\tilde{\pi}\delta_{ij} + T_{ij}^0 = -\tilde{\pi}\delta_{ij} + 2d_{ij},$$

where $\tilde{\pi}$ is the fluid pressure, and T_{ij}^0 is the symmetric extra stress which depends only on d_{ij}. Notice that usually there is a coefficient μ, representing the dynamic viscosity, in front of d_{ij} but this is normalized due to our nondimensionalization. To handle the extra complexity of the second gradients of u_i, [27] and [28] introduce a third-order tensor which [27] refer to as a hyperstress, G_{ijk}, which has the form

$$G_{ijk} = -\tilde{\pi}_k\delta_{ij} + G_{ijk}^0, \tag{8}$$

where $\tilde{\pi}_k$ is a pressure vector and G_{ijk}^0 is the extra hyperstress involving only $u_{i,jk}$. To incorporate the extra complexity involved with the third gradients of u_i, [28] introduces a fourth-order tensor H_{ijkh} of the form

$$H_{ijkh} = -\delta_{ij}\Pi_{kh} + H_{ijkh}^0,$$

where Π_{kh} is a pressure tensor and H_{ijkh}^0 is the fourth-order extra stress which involves only $u_{i,jkh}$.

The total stress which arises in Equation (5) is $\sigma_{ij} = T_{ij} - G_{ijk,k} + H_{ijkh,hk}$ and this yields the terms $-\pi_{,i} + \Delta u_i - \xi\Delta^2 u_i + \gamma\Delta^3 u_i$, that is, in Equation (5),

$$\sigma_{ij,j} = -\pi_{,i} + \Delta u_i - \xi\Delta^2 u_i + \gamma\Delta^3 u_i = (T_{ij} - G_{ijk,k} + H_{ijkh,hk})_{,j}, \tag{9}$$

where $\pi = \tilde{\pi} + \tilde{\pi}_{k,k} + \Pi_{kh,hk}$ is the total pressure.

Musesti [28, p. 87] writes: "*A discussion about boundary conditions of third order fluids [...] would be desirable.*" To analyze thermal convection, it is essential and so we now do this. To develop a complete set of boundary conditions, we commence by multiplying $\sigma_{ij,j}$ by u_i and integrate over the domain Ω. Let $\|\cdot\|$ and $(\cdot,\cdot)$ denote the norm and inner product on $L^2(\Omega)$. Throughout, we suppose we have no-slip boundary conditions so that $u_i = 0$ on Γ. Under these conditions, $(u_i, \pi_{,i}) = -(u_{i,i}, \pi) = 0$. Hence, we obtain after integration by parts and use of the boundary conditions on u_i,

$$(\sigma_{ij,j}, u_i) = -(\sigma_{ij}, u_{i,j}) = -(T_{ij}^0, u_{i,j}) + (G_{ijk,k}^0, u_{i,j}) - (H_{ijkh,hk}^0, u_{i,j}). \tag{10}$$

We deal with each integral on the right of (10) below. First,

$$-(T_{ij}^0, u_{i,j}) = -2(d_{ij}, u_{i,j}) = -\|\nabla\mathbf{u}\|^2. \tag{11}$$

Second,

$$(G_{ijk,k}^0, u_{i,j}) = -(G_{ijk}^0, u_{i,jk}) + \oint_\Gamma G_{ijk}^0 n_k u_{i,j}\,dA, \tag{12}$$

where dA denotes the element of integration over Γ.

To handle the boundary term, we follow the notation of [59] and we denote with $\alpha = 1, 2$ the indices with respect to the two surface coordinates on Γ and let $a^{\alpha\beta}$ be the fundamental surface tensor for the surface Γ. This allows one to write on Γ,

$$u_{i,j} = n_j\frac{\partial u_i}{\partial n} + x_{j;\alpha}a^{\alpha\beta}u_{i;\beta}, \tag{13}$$

where $;\alpha$ denotes surface covariant differentiation, that is, it allows one to split $u_{i,j}$ into components normal to the surface Γ, and tangential to this surface. Since $u_i \equiv 0$ on Γ, the tangential components, which are derivatives along the directions

of the surface coordinates, are zero. Hence, (12) becomes

$$(G_{ijk,k}^0, u_{i,j}) = -(G_{ijk}^0, u_{i,jk}) + \oint_\Gamma m_i \frac{\partial u_i}{\partial n}\, dA\,, \tag{14}$$

where

$$m_i = G_{ijk}^0 n_k n_j\,. \tag{15}$$

We now employ integration by parts to derive an expression for the H_{ijkh} term. We may derive

$$-(H_{ijkh,hk}^0, u_{i,j}) = (H_{ijkh,h}^0, u_{i,jk}) - \oint_\Gamma H_{ijkh,h}^0 n_k n_j \frac{\partial u_i}{\partial n}\, dA = -(H_{ijkh}^0, u_{i,jkh}) + \oint_\Gamma H_{ijkh}^0 u_{i,jk} n_h dA - \oint_\Gamma H_{ijkh,h} n_k n_j \frac{\partial u_i}{\partial n}\, dA\,. \tag{16}$$

Treatment of the second integral on the right of (16) is quite involved. We repeatedly use the decomposition (13) into normal and tangential components on Γ. Write

$$I = \oint_\Gamma H_{ijkh}^0 u_{i,jk} n_h\, dA = I_1 + I_2, \tag{17}$$

where

$$I_1 = \oint_\Gamma H_{ijkh}^0 n_h \frac{\partial}{\partial n}(u_{i,j}) n_k\, dA\,, \tag{18}$$

and

$$I_2 = \oint_\Gamma H_{ijkh}^0 n_h x_{k;\alpha} a^{\alpha\beta} (u_{i,j})_{;\beta}\, dA\,. \tag{19}$$

The term I_1 is written as

$$\begin{aligned}
I_1 &= \oint_\Gamma H_{ijkh}^0 n_k n_h n_q u_{i,jq} dA \\
&= \oint_\Gamma H_{ijkh}^0 n_k n_h n_q (u_{i,q})_{,j} dA \\
&= \oint_\Gamma H_{ijkh}^0 n_k n_h n_q \frac{\partial}{\partial n}(u_{i,q}) n_j\, dA + \oint_\Gamma H_{ijkh}^0 n_k n_h n_q\, x_{j;\alpha} a^{\alpha\beta}(u_{i,q})_{;\beta}\, dA.
\end{aligned}$$

Then,

$$I = \oint_\Gamma H_{ijkh}^0 n_j n_k n_h \frac{\partial^2 u_i}{\partial n^2}\, dA + J_1 + J_2\,,$$

where

$$J_1 = \oint_\Gamma H_{ijkh}^0 n_h x_{k;\alpha} a^{\alpha\beta}(u_{i,j})_{;\beta}\, dA,$$

$$J_2 = \oint_\Gamma H_{ijkh}^0 n_h n_k n_q\, x_{j;\alpha} a^{\alpha\beta}(u_{i,q})_{;\beta}\, dA.$$

This procedure leads to

$$J_1 = -\oint_\Gamma H_{ijkh,m}^0 n_h x_{m;\beta} x_{k;\alpha} a^{\alpha\beta} u_{i,j}\, dA - \oint_\Gamma H_{ijkh}^0 n_{h;\beta} x_{k;\alpha} a^{\alpha\beta} u_{i,j} dA - \oint_\Gamma H_{ijkh}^0 n_h x_{k;\alpha\beta} a^{\alpha\beta} u_{i,j} dA.$$

We now need to employ the Gauss equations $x_{i;\alpha\beta} = b_{\alpha\beta}n_i$ and the Gauss–Weingarten relations $n_{i;\alpha} = -b_\alpha^\beta x_{i;\beta}$, where $b_{\alpha\beta}$ arises in the second fundamental form of the surface Γ. In this way, we derive

$$J_1 = -\oint_\Gamma H^0_{ijkh,m} n_h x_{m;\beta} x_{k;\alpha} a^{\alpha\beta} u_{i,j}\, dA + \oint_\Gamma H^0_{ijkh} b_\beta^\xi x_{h;\xi} x_{k;\alpha} a^{\alpha\beta} u_{i,j}\, dA - \oint_\Gamma H^0_{ijkh} n_h n_k b_\alpha^\alpha u_{i,j}\, dA, \tag{20}$$

where $2H = b_\alpha^\alpha = a^{\alpha\beta} b_{\alpha\beta}$ is twice the mean curvature of the surface Γ. A similar calculation with J_2 leads to

$$
\begin{aligned}
J_2 = & -\oint_\Gamma H^0_{ijkh,m} n_k n_h n_q\, x_{m;\beta} x_{j;\alpha} a^{\alpha\beta} u_{i,q}\, dA \\
& -\oint_\Gamma H^0_{ijkh} x_{j;\alpha} \left[n_{k;\beta} n_h n_q + n_k n_q n_{h;\beta} + n_k n_h n_{q;\beta} \right] a^{\alpha\beta} u_{i,q}\, dA \\
& -\oint_\Gamma H^0_{ijkh} n_k n_h n_q x_{j;\alpha\beta} a^{\alpha\beta} u_{i,q}\, dA \\
= & -\oint_\Gamma H^0_{ijkh,m} n_k n_h x_{m;\beta} x_{j;\alpha} a^{\alpha\beta} \frac{\partial u_i}{\partial n}\, dA \\
& +\oint_\Gamma H^0_{ijkh} x_{j;\alpha} \left[b_\beta^\xi x_{k;\xi} n_h + b_\beta^\xi x_{h;\xi} n_k \right] a^{\alpha\beta} \frac{\partial u_i}{\partial n}\, dA \\
& +\oint_\Gamma H^0_{ijkh} b_\beta^\xi x_{q;\xi} a^{\alpha\beta} n_k n_h x_{j;\alpha} u_{i,q}\, dA \\
& -\oint_\Gamma H^0_{ijkh} b_\alpha^\alpha n_k n_h n_j \frac{\partial u_i}{\partial n}\, dA.
\end{aligned}
\tag{21}
$$

We now use expression (13) in (20) and (21) and recognize that the tangential parts of $u_{i,q}$ yield zero contribution. In this way, combining (16), (17), (18), (19), (20), and (21), we may see that

$$-(H^0_{ijkh,hk}, u_{i,j}) = -(H^0_{ijkh}, u_{i,jkh}) + \oint_\Gamma h_i \frac{\partial^2 u_i}{\partial n^2}\, dA + \oint_\Gamma q_i \frac{\partial u_i}{\partial n}\, dA, \tag{22}$$

where

$$
\begin{aligned}
q_i = & -H^0_{ijkh,h} n_k n_j - H^0_{ijkh,m} n_j n_h a^{\alpha\beta} x_{m;\beta} x_{k;\alpha} \\
& -H^0_{ijkh,m} n_k n_h a^{\alpha\beta} x_{m;\beta} x_{j;\alpha} + H^0_{ijkh} b^{\xi\alpha} x_{h;\xi} x_{k;\alpha} n_j \\
& -H^0_{ijkh} n_h n_k n_j b_\alpha^\alpha + H^0_{ijkh} x_{j;\alpha} b_\beta^\xi (n_h x_{k;\xi} + n_k x_{h;\xi}) a^{\alpha\beta} \\
& +H^0_{ijkh} n_k n_h n_q x_{j;\alpha} x_{q;\xi} b^{\xi\alpha} - H^0_{ijkh} b_\alpha^\alpha n_k n_h n_j.
\end{aligned}
\tag{23}
$$

Finally, we obtain from (10), (11), (14), and (22),

$$(\sigma_{ij,j}, u_i) = -\|\nabla \mathbf{u}\|^2 - (G^0_{ijk}, u_{i,jk}) - (H^0_{ijkh}, u_{i,jkh}) + \oint_\Gamma h_i \frac{\partial^2 u_i}{\partial n^2}\, dA + \oint_\Gamma p_i \frac{\partial u_i}{\partial n}\, dA, \tag{24}$$

where

$$h_i = H^0_{ijkh} n_j n_k n_h \qquad \text{and} \qquad p_i = m_i + q_i.$$

To employ (24) in practice, we need expressions for G^0_{ijk} and H^0_{ijkh} and these are given by [28]. They have the form

$$G^0_{ijk} = \eta_1 u_{i,jk} + \eta_2 (u_{j,ik} + u_{k,ij} - \delta_{jk} \Delta u_i) + \eta_3 (\delta_{ij} \Delta u_k + \delta_{ik} \Delta u_j - 4\delta_{jk} \Delta u_i), \tag{25}$$

and

$$
\begin{aligned}
H^0_{ijkh} = &\,\mathfrak{A}(\delta_{ij}[\Delta u_{k,h} + \Delta u_{h,k}] + \delta_{ik}[\Delta u_{j,h} + \Delta u_{h,j}] + \delta_{ih}[\Delta u_{k,j} + \Delta u_{j,k}]) \\
&+ \mathfrak{D}(\delta_{jk}\Delta u_{i,h} + \delta_{jh}\Delta u_{i,k} + \delta_{kh}\Delta u_{i,j}) \\
&+ \mathfrak{E}u_{i,jkh} + \mathfrak{F}(\delta_{kh}\Delta u_{j,i} + \delta_{jk}\Delta u_{h,i} + \delta_{jh}\Delta u_{k,i}) \\
&+ \mathfrak{G}(u_{j,ikh} + u_{k,ijh} + u_{h,ijk}).
\end{aligned}
\tag{26}
$$

The coefficients η_1, η_2, and η_3 satisfy the relation

$$
\xi = \eta_1 - \eta_2 - 4\eta_3 \geq 0,
$$

and, by identifying 18 individual components and a very clever splitting of the matrix in a quadratic form, in [30] the optimal conditions for the dissipation inequality are given:

$$
\eta_1 + 2\eta_2 \geq 0, \qquad \eta_1 - \eta_2 \geq 0, \qquad \eta_1 - \eta_2 - 6\eta_3 - 2\sqrt{\eta_2^2 + 4\eta_2\eta_3 + 9\eta_3^2} \geq 0.
$$

The coefficients $\mathfrak{A}, \mathfrak{D}, \mathfrak{E}, \mathfrak{F}$, and $\mathfrak{G}$ satisfy

$$
\gamma = 3\mathfrak{D} + \mathfrak{E} \geq 0.
$$

We may now define various classes of boundary conditions for a sixth-order fluid. We define $h_i = H_{ijkh}n_j n_k n_h$. We only deal with no-slip conditions, and we say that the boundary conditions are of *strong adherence* type if

$$
u_i = 0, \; \frac{\partial u_i}{\partial n} = 0, \; \frac{\partial^2 u_i}{\partial n^2} = 0 \qquad \text{on } \Gamma.
$$

They are of *weak adherence* type if

$$
u_i = 0, \; \frac{\partial u_i}{\partial n} = 0, \; h_i = 0 \qquad \text{on } \Gamma.
$$

They are of *general adherence* type if

$$
u_i = 0, \; \frac{\partial u_i}{\partial n} = 0, \; h_i = -\ell \frac{\partial^2 u_i}{\partial n^2} \qquad \text{on } \Gamma,
$$

where $\ell > 0$ is a constant to be prescribed.

In this work, we concentrate on the above three types of boundary conditions and we refer to these as cases I, II and III, respectively.

The sixth-order theory presented in [28] has a richer structure, and one may define a further four types of no-slip boundary conditions. These are

$$
u_i = 0, \; h_i = 0, \; p_i = 0 \qquad \text{on } \Gamma,
$$

then for a constant $\ell_1 > 0$,

$$
u_i = 0, \; h_i = -\ell_1 \frac{\partial^2 u_i}{\partial n^2}, \; p_i = 0 \qquad \text{on } \Gamma,
$$

or for a constant $\ell_2 > 0$,

$$
u_i = 0, \; h_i = 0, \; p_i = -\ell_2 \frac{\partial u_i}{\partial n}, \qquad \text{on } \Gamma,
$$

and

$$u_i = 0, \ h_i = -\ell_1 \frac{\partial^2 u_i}{\partial n^2}, \ p_i = -\ell_2 \frac{\partial u_i}{\partial n} \qquad \text{on } \Gamma.$$

We do not treat the latter four classes of boundary conditions in the context of thermal convection, they involve explicit values of the Musesti coefficients $\eta_1, \eta_2, \eta_3, \mathfrak{A}, \mathfrak{D}, \mathfrak{E}, \mathfrak{F}$, and $\mathfrak{G}$. However, these boundary conditions should prove to be of importance in microfluidic situations and will be the subject of future work. We finally mention that one could also produce a further class of boundary conditions corresponding to the stress vector being zero on a surface Γ. The necessary details may be worked out in a similar manner to the above.

5 | Nonlinear Stability

We now focus on the Musesti model and collect the perturbation equations. We recall that system (5) gives

$$\begin{aligned}
&u_{i,t} + u_j u_{i,j} = -\pi_{,i} + R\theta k_i + \Delta u_i - \xi \Delta^2 u_i + \gamma \Delta^3 u_i, \\
&u_{i,i} = 0, \\
&Pr(\theta_{,t} + u_i \theta_{,i}) = Rw + \Delta\theta,
\end{aligned} \qquad (27)$$

where π collects the contributions of $\tilde{\pi}$, $\tilde{\pi}_k$, and Π_{jk}.

Equations (27) are defined on the domain $\mathbb{R}^2 \times \{z \in (0,1)\} \times \{t > 0\}$. Denote by $\| \cdot \|$ and $(\cdot, \cdot)$ the norm and inner product on $L^2(V)$. We now rewrite system (27), together with any of the boundary conditions I, II, or III, in the form of an abstract operator equation

$$BU_t + LU + N(U) = 0, \qquad (28)$$

where $U = (u, v, w, \theta, \pi)^T$ and where B is a linear symmetric operator, L is an unbounded linear operator and $N(U)$ represents the nonlinear terms, defined on a dense domain of the Hilbert space $H = [L^2(V)]^4$ (cf. [60, pp. 212–215]). In the present case, the operator B has form $B = diag\{1, 1, 1, Pr, 0\}$, the nonlinearities $N(U)$ consist of $u_j u_{i,j}$ and $u_i \theta_{,i}$, while L is represented by the right-hand side of (27). The solution is understood to be periodic in x, y and the components of u_i in addition to being zero on $z = 0, 1$ also satisfy boundary conditions of case I, II, or III.

We start by deriving a general energy equality. We multiply $(27)_1$ by u_i and integrate over V and then multiply $(27)_3$ by θ and integrate over V. Upon employing the boundary condition I or II, we may obtain the energy equation

$$\frac{d}{dt}\left(\frac{1}{2}\|\mathbf{u}\|^2 + \frac{Pr}{2}\|\theta\|^2\right) = 2R(\theta, w) - \|\nabla\mathbf{u}\|^2 - \|\nabla\theta\|^2 - Y, \qquad (29)$$

where the stabilizing term involving the second and third spatial gradients is defined by

$$Y = (G^0_{ijk}, u_{i,jk}) + (H^0_{ijkh}, u_{i,jkh}).$$

In the situation where boundary conditions III are employed, it is necessary to add

$$-\ell \oint_{\partial V} \frac{\partial^2 u_i}{\partial n^2} \frac{\partial^2 u_i}{\partial n^2} \, dA$$

to the right-hand side of (29).

The tensors G^0_{ijk} and H^0_{ikjh} are given in (25) and (26) and it is useful to introduce the symmetric and skew-symmetric parts of $u_{i,j}$:

$$d_{ij} = \frac{1}{2}(u_{i,j} + u_{j,i}), \qquad \omega_{ij} = \frac{1}{2}(u_{i,j} - u_{j,i}).$$

We can now rewrite Y (i.e., the higher-order gradient term) as

$$
\begin{aligned}
Y ={}& \eta_1(u_{i,jk}, u_{i,jk}) + 2\eta_2 \left[(d_{ij,k}, d_{ij,k}) - (\omega_{ij,k}, \omega_{ij,k}) \right] - (\eta_2 + 4\eta_3)\|\Delta\mathbf{u}\|^2 \\
&+ 3\mathfrak{D}(\Delta u_{i,k}, \Delta u_{i,k}) + \mathfrak{E}(u_{i,jkh}, u_{i,jkh}) + 3\mathfrak{F}(\Delta u_{i,j}, \Delta u_{j,i}) + 3\mathfrak{G}(u_{i,jkh}, u_{j,ikh}), \\
={}& (\eta_1 + 2\eta_2)(d_{ij,k}, d_{ij,k}) + (\eta_1 - 2\eta_2)(\omega_{ij,k}, \omega_{ij,k}) - (\eta_2 + 4\eta_3)\|\Delta\mathbf{u}\|^2 \\
&+ 3(\mathfrak{D} + \mathfrak{F})(\Delta d_{ij}, \Delta d_{ij}) + 3(\mathfrak{D} - \mathfrak{F})(\Delta\omega_{ij}, \Delta\omega_{ij}) \\
&+ (\mathfrak{E} + 3\mathfrak{G})(d_{ij,kh}, d_{ij,kh}) + (\mathfrak{E} - 3\mathfrak{G})(\omega_{ij,kh}, \omega_{ij,kh}).
\end{aligned}
\tag{30}
$$

The right-hand side of (29) together with (30) allows us to introduce a bilinear form on H. Let $U = (u^1, v^1, w^1, \theta, \pi^1)^T$ and $W = (u^2, v^2, w^2, \phi, \pi^2)^T$ be solutions to (27) subject to boundary conditions of case I, II, or III. Let d_{ij}, ω_{ij} be the symmetric and skew-symmetric parts of $u^1_{i,j}$, and let e_{ij}, ζ_{ij} be the symmetric and skew-symmetric parts of $u^2_{i,j}$. Then define a bilinear form on H by

$$
\begin{aligned}
(W, LU) ={}& 2R \left[(w^2, \theta) + (w^1, \phi) \right] - (\nabla\mathbf{u}^1, \nabla\mathbf{u}^2) - (\nabla\theta, \nabla\phi) \\
&- (\eta_1 + 2\eta_2)(d_{ij,k}, e_{ij,k}) - (\eta_1 - 2\eta_2)(\omega_{ij,k}, \zeta_{ij,k}) \\
&+ (\eta_2 + 4\eta_3)(\Delta\mathbf{u}^1, \Delta\mathbf{u}^2) - 3(\mathfrak{D} + \mathfrak{F})(\Delta d_{ij}, \Delta e_{ij}) \\
&- 3(\mathfrak{D} - \mathfrak{F})(\Delta\omega_{ij}, \Delta\zeta_{ij}) - (\mathfrak{E} + 3\mathfrak{G})(d_{ij,kh}, e_{ij,kh}) \\
&- (\mathfrak{E} - 3\mathfrak{G})(\omega_{ij,kh}, \zeta_{ij,kh}) - \ell \oint_{\partial V} \frac{\partial^2 \mathbf{u}^1}{\partial n^2} \cdot \frac{\partial^2 \mathbf{u}^2}{\partial n^2} \, dA \,,
\end{aligned}
\tag{31}
$$

where the boundary term is present in case III, but is not present for cases I and II.

We have that L is a symmetric operator, because one can easily prove that $(W, LU) = (U, LW)$.

Moreover,

$$
(U, N(U)) = (u_j u_{i,j}, u_i) + (u_i \theta_{,i}, \theta) = 0,
$$

as may be seen by integration by parts, the fact that $u_{i,i} = 0$, and use of the boundary conditions, and the resulting nonlinear stability is global. Therefore, following [60], we have that the linear threshold for instability is equal to the threshold for nonlinear stability. Actually, this may also be seen by examining the linear theory and showing that the growth rate is zero. In particular, denoting by σ the growth rate in a representation of time like $e^{\sigma t}$ and the complex conjugate of U by U^*, we have $\sigma(U^*, BU) = (U^*, LU)$ which gives $\mathrm{Im}\,\sigma = 0$. Then, the energy equation can be adjusted and one can determine the critical Rayleigh number for nonlinear energy stability by using the dissipation terms and the maximum of the production. With this procedure, one obtains the same Euler–Lagrange equations that appear in the linear instability equations. Nevertheless, the main finding is that the nonlinear stability issue can be fully captured by determining the threshold of instability through linear instability theory.

Remark. Regarding case I, the domain $D(L)$ of the operator L consists of $\{\mathbf{u} \in (W_0^{3,2}(V))^3\} \times \{\theta \in W_0^{1,2}(V)\}$ and the relevant functional spaces for addressing the existence and uniqueness of a solution are analogous to those carefully introduced by [29, Section 7.2.2] for a similar problem, which considers only the second and fourth derivatives. Existence and uniqueness of a solution in case I can be established by following the approach in [61], with the key modification of adding a third Laplacian to the fluid equation and dropping the bi-Laplacian term in the temperature equation, using the analytical techniques outlined in [29]. For cases II and III, existence theory becomes more complicated: proving existence and uniqueness under these boundary conditions would shift the focus of this paper, which aims to provide a concise yet comprehensive analysis of the problem. This aspect will be addressed in a forthcoming study. However, in the interests of analyzing convection scenarios within the current model, we study here the impact of these cases on the stability.

6 | Assessment of the Critical Rayleigh Number Associated With Instability

The standard approach to determine the critical Rayleigh numbers for instability involves linearizing (27) and searching for solutions of the form

$$u_i = u_i(\mathbf{x})e^{\sigma t}, \qquad \theta = \theta(\mathbf{x})e^{\sigma t}, \qquad \pi = \pi(\mathbf{x})e^{\sigma t}.$$

Here, we follow this approach, noting that since $\sigma \in \mathbb{R}$, the threshold for linear stability occurs at $\sigma = 0$. We proceed by linearizing, setting $\sigma = 0$, and then applying the curl–curl operator to $(27)_1$ to eliminate π. Retaining only the third component of the resulting expression, we arrive at the following system that must be solved:

$$0 = -\Delta^2 w + \xi \Delta^3 w - \gamma \Delta^4 w - R\Delta^* \theta,$$

$$0 = Rw + \Delta\theta,$$

where $\Delta^* = \partial^2/\partial x^2 + \partial/\partial y^2$. We solve this system numerically using a Chebyshev tau method. It is preferable to work with the following equivalent system to mitigate issues with spurious eigenvalues:

$$0 = -\Delta^2 w + \xi \Delta^3 w - \gamma \Delta^4 w - R^2 \Delta^* \theta,$$

$$0 = w + \Delta\theta,$$

(32)

where $R^2 = Ra$. The system will be solved with the following boundary conditions, corresponding to cases I, II, and III.

6.1 | Boundary Conditions for Case I

Here,

$$u_i = 0, \quad \frac{\partial u_i}{\partial n} = 0, \quad \frac{\partial^2 u_i}{\partial n^2} = 0, \qquad \text{on } z = 0, 1, \ i = 1, 2, 3,$$

while periodic boundary conditions are applied along the lateral walls of the cell V. Hence,

$$w = 0, \quad w_z = 0, \quad w_{zz} = 0, \quad u_{zz} = 0, \quad v_{zz} = 0, \qquad \text{on } z = 0, 1.$$

Due to the fact that $u_x + v_y + w_z = 0$ in V, then we have (on $z = 0, 1,$):

$$u_{xzz} + v_{yzz} + w_{zzz} = 0,$$

hence $w_{zzz} = 0$ on $z = 0, 1$. Thus, the following are the boundary conditions for case I:

$$w = w_z = w_{zz} = w_{zzz} = 0, \qquad z = 0, 1.$$

(33)

6.2 | Boundary Conditions for Case II

In this case,

$$u_i = 0, \qquad \frac{\partial u_i}{\partial n} = 0, \qquad h_i = 0, \qquad \text{on } z = 0, 1,$$

where $i = 1, 2, 3$ and $h_i = H_{ijkh} n_j n_k n_h$ with $\mathbf{n} = (0, 0, 1)$. Since

$$w = 0, w_z = 0, u_z = 0, v_z = 0 \qquad \text{on } z = 0, 1,$$

and **u** is solenoidal, it follows that

$$w = 0, w_z = 0, w_{zz} = 0 \qquad \text{on } z = 0, 1.$$

In addition for $h_\alpha = 0$, $\alpha = 1, 2$, we find on $z = 0, 1$,

$$h_\alpha = H^0_{\alpha333} = 3\mathfrak{D}\Delta u_{\alpha,z} + \mathfrak{E}u_{\alpha,zzz} + 3\mathfrak{F}\Delta w_{,\alpha} + 3\mathfrak{G}w_{,zz\alpha} = 0, \quad \text{on } z = 0, 1.$$

Differentiate the equation for $\alpha = 1$ by x, differentiate the equation for $\alpha = 2$ by y, and then use the continuity equation to see that on $z = 0, 1$,

$$-(3\mathfrak{D} + \mathfrak{E})w_{zzzz} + 3(\mathfrak{F} + \mathfrak{G} - \mathfrak{D})\Delta^* w_{zz} = 0.$$

Since $w_{zz} = 0$ on $z = 0, 1$, it follows that $w_{zzzz} = 0$ there. Hence the boundary conditions for case II are

$$w = w_z = w_{zz} = w_{zzzz} = 0, \qquad z = 0, 1. \tag{34}$$

Remark. To determine the pressure vector component Π_{33}, the boundary condition $h_3 = 0$ is used.

6.3 | Boundary Conditions for Case III

Here,

$$u_i = 0, \qquad \frac{\partial u_i}{\partial n} = 0, \qquad h_i = -\ell\,\frac{\partial^2 u_i}{\partial n^2}, \qquad \text{on } z = 0, 1,$$

where $i = 1, 2, 3$ and

$$h_i = H_{ijkh}n_j n_k n_h = H_{i333} = -\Pi_{33,3i} + 6\mathfrak{A}\delta_{i3}\Delta w_{,3} + 3\mathfrak{D}\Delta u_{i,3} + \mathfrak{E}u_{i,333} + 3\mathfrak{F}\Delta w_{,i} + 3\mathfrak{G}w_{,33i}.$$

Using h_1, h_2, and the continuity equation, we can apply similar reasoning as above to demonstrate that the general adherence boundary conditions are

$$w = w_z = w_{zz} = 0, \qquad \gamma w_{zzzz} + \ell w_{zzz} = 0,$$

on $z = 0, 1$. Therefore, the general adherence boundary conditions are

$$w = 0, \quad w_z = 0, \quad w_{zz} = 0, \quad w_{zzzz} + q w_{zzz} = 0, \qquad \text{on } z = 0, 1, \tag{35}$$

where $q = \ell/\gamma > 0$.

7 | Numerical Methods and Numerical Results

To solve Equations (32) under boundary conditions I–III, we use a Chebyshev tau method (see [62]). For this, we express

$$w = W(z)h(x, y), \quad \theta = \Theta(z)h(x, y),$$

where h satisfies $\Delta^* h = -a^2 h$, where a is a wavenumber.

We solve (32) for the eigenvalues Ra by writing these equations as a system

$$(D^2 - a^2)W = \chi,$$

$$(D^2 - a^2)\chi = \psi,$$

$$(D^2 - a^2)\psi = \eta,$$

$$(D^2 - a^2)\eta + \frac{1}{\gamma}\psi - \frac{\xi}{\gamma}\eta = Ra\,\frac{a^2}{\gamma}\,\Theta,$$

$$(D^2 - a^2)\Theta + W = 0, \tag{36}$$

where $D = d/dz$. The boundary conditions may now be written in the form

Case I	$\Theta = W = DW = \chi = D\chi = 0,$	$z = 0, 1,$
Case II	$\Theta = W = DW = \chi = \psi = 0,$	$z = 0, 1,$
Case III	$\Theta = W = DW = \chi = 0, \quad \psi + qD\chi = 0,$	$z = 0, 1.$

The solution to (36) is expressed as a sum of Chebyshev polynomials in the form

$$W = \sum_{i=0}^{N} W_i T_i(z),$$

$$\chi = \sum_{i=0}^{N} \chi_i T_i(z),$$

$$\psi = \sum_{i=0}^{N} \psi_i T_i(z),$$

$$\eta = \sum_{i=0}^{N} \eta_i T_i(z),$$

$$\Theta = \sum_{i=0}^{N} \Theta_i T_i(z).$$

This generates a generalized matrix eigenvalue problem of the following form:

$$A\mathbf{x} = Ra\,B\mathbf{x},$$

where

$$\mathbf{x} = (W_0, \dots, W_N, \chi_0, \dots, \chi_N, \psi_0, \dots, \psi_N, \eta_0, \dots, \eta_N, \Theta_0, \dots, \Theta_N).$$

The boundary conditions are directly integrated into the appropriate rows of the system matrix A. The resulting matrix eigenvalue problem is then solved using the QZ algorithm of [63].

We now report on numerical results for Equations (27). The values of ξ and γ selected are chosen to display the type of behavior witnessed. The typical new behavior is found for γ very small, while ξ is also small it is comparatively larger. For larger values of the parameters displayed here the stabilizing effects are seen with very large values of critical Rayleigh number. Numerical results for boundary conditions of type I are given in Table 1 whereas those for boundary conditions of type II are included in Table 2. Figures 1 and 2 show graphical output for the critical Rayleigh number and for the critical wavenumber for strong and weak adherence boundary conditions. It is seen that for the strong adherence boundary conditions, case I, the critical Rayleigh number increases strongly for γ as shown in the first five values of Table 1, whereas the growth of the Rayleigh number is still increasing but at a much lesser rate when the variation is in ξ, as seen by comparison with the next six values in Table 1. Clearly, the γ term which represents the tri-Laplacian has a stronger stabilizing effect than the ξ term which is for the bi-Laplacian. Physically, this is to be expected. The dominance of γ over ξ continues to be observed in Table 2 which is for weak adherence boundary conditions, although the rate of growth in the critical values of Ra is less pronounced.

TABLE 1 | Critical Rayleigh and wave numbers for boundary conditions of Case I, strong adherence, versus γ, ξ. The classical values which hold for $\gamma = 0, \xi = 0$ and fixed surfaces are $R = 1707.76$, $a^2 = 9.712$.

Ra	a^2	γ	ξ
1707.76	9.712	0	0
2020.22	10.53	10^{-7}	0
2333.33	11.00	10^{-6}	0
3155.21	12.13	10^{-5}	0
7009.72	13.70	10^{-4}	0
3155.23	12.13	10^{-5}	10^{-7}
3155.42	12.13	10^{-5}	10^{-6}
3157.35	12.13	10^{-5}	10^{-5}
3176.66	12.13	10^{-5}	10^{-4}
3368.79	12.16	10^{-5}	10^{-3}
5236.80	12.28	10^{-5}	10^{-2}
3155.42	12.13	10^{-6}	10^{-5}
3157.35	12.13	10^{-5}	10^{-5}
7012.21	13.70	10^{-4}	10^{-5}

TABLE 2 | Critical Rayleigh and wave numbers for boundary conditions of Case II, weak adherence, versus γ, ξ. The classical values which hold for $\gamma = 0, \xi = 0$ and fixed surfaces are $R = 1707.76$, $a^2 = 9.712$.

Ra	a^2	γ	ξ
2032.77	10.36	10^{-6}	0
2476.26	10.85	10^{-5}	0
4482.71	11.36	10^{-4}	0
2476.45	10.85	10^{-5}	10^{-6}
2495.50	10.87	10^{-5}	10^{-4}
2667.65	10.97	10^{-5}	10^{-3}
4346.97	11.47	10^{-5}	10^{-2}

The behavior of the critical wavenumber for cases I and II is shown in Tables 1 and 2, and in Figures 1 and 2. In both cases, the critical wavenumber rises as γ increases. This means that since the wavenumber is inversely proportional to the aspect ratio of the convection cell (width to depth), increasing γ means the cells become narrower for a fixed depth. The presence of the tri-Laplacian appears to concentrate the convection cells more together to produce a smaller pattern when viewed from above.

For the general adherence boundary conditions with $q = \ell/\gamma$, Figures 3 and 4 and Table 3 show the critical Rayleigh number varies from the weak adherence value at $q = 0$ ($\ell = 0$), to the strong adherence value as q increases ($\ell \to \infty$). The variation is from $Ra = 2476$ to $Ra = 3155$ when $\gamma = 10^{-5}, \xi = 0$, with a^2 increasing from 10.85 to 12.13 over the same range. The variation is from $Ra = 4347$ to $Ra = 5237$ when $\gamma = 10^{-5}, \xi = 10^{-2}$, with a^2 increasing from 11.47 to 12.28 over the same range.

8 | Conclusions

In this paper, we have investigated a model for thermal convection in a higher-order Navier–Stokes theory, introduced for isothermal flow by [28]. In the model, the stress depends on spatial velocity gradients up to third-order derivatives, so that the associated PDE is of sixth order. This kind of fluids are physically relevant, since the presence of such extra spatial
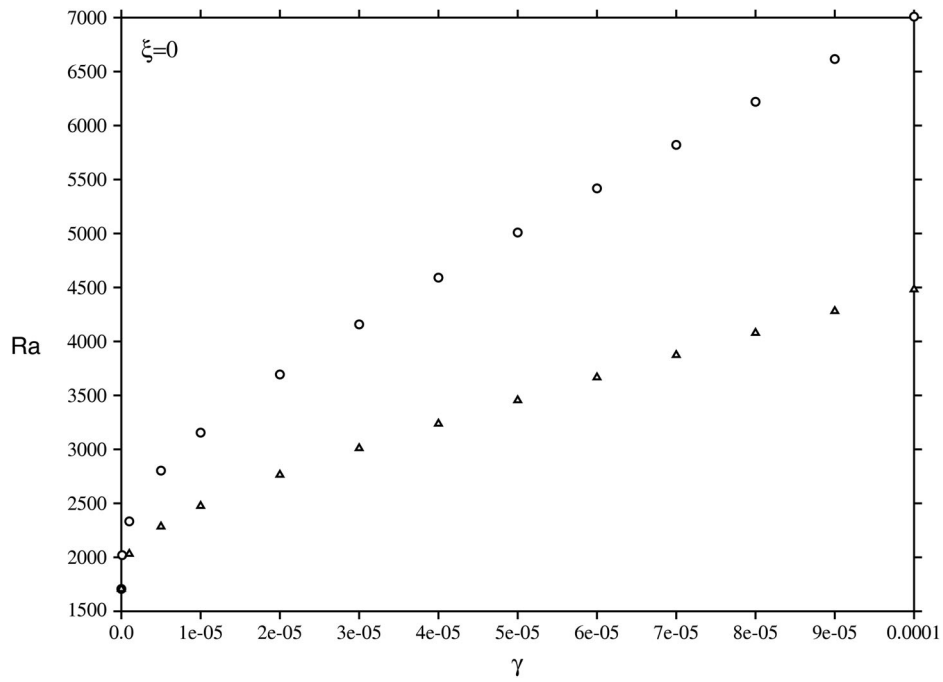
FIGURE 1 | Graph of Ra versus γ, case I boundary conditions, strong adherence are open circles, case II boundary conditions, weak adherence are triangles; $\xi = 0$. The value of Ra when $\gamma = 0, \xi = 0$ is 1707.76.
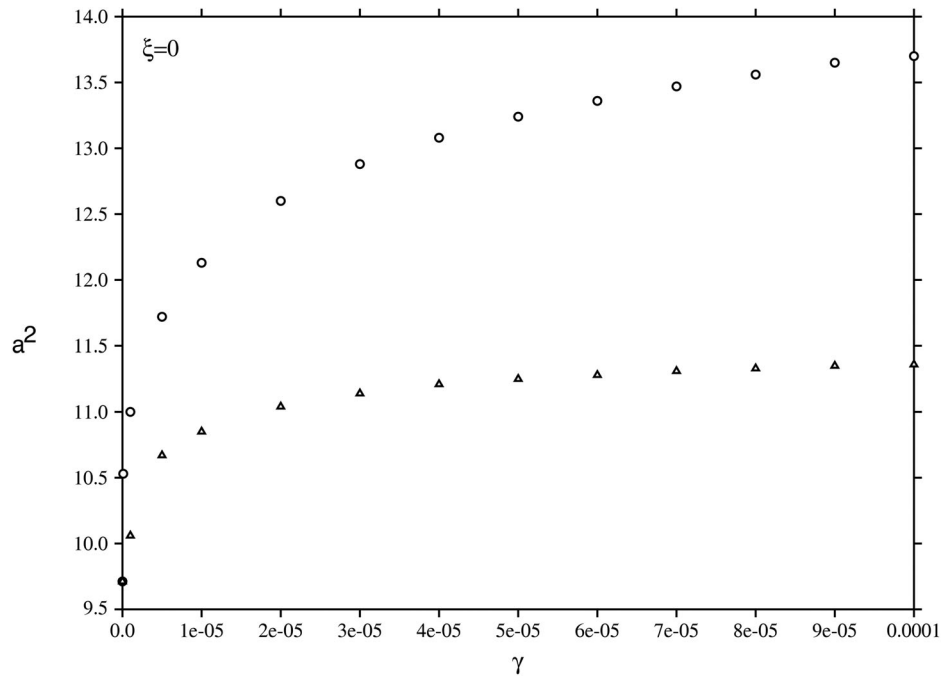

FIGURE 2 | Graph of a^2 versus γ, case I boundary conditions, strong adherence are open circles, case II boundary conditions, weak adherence are triangles; $\xi = 0$. The value of a^2 when $\gamma = 0, \xi = 0$ is 9.712.

derivatives can capture, for instance, some features of the flow when the composition of the fluid involves long molecules, or in applications to microfluidic industry where length scales are very small (see [27, 64–66]).

By including also temperature into the model, we have studied the Bénard thermal convection problem, employing meaningful boundary conditions, which have been derived up to the highest order. We have shown that linear instability provides the same results of a global nonlinear energy stability analysis; this is an optimal result and shows that linear instability theory is enough to capture the physics of the problem.
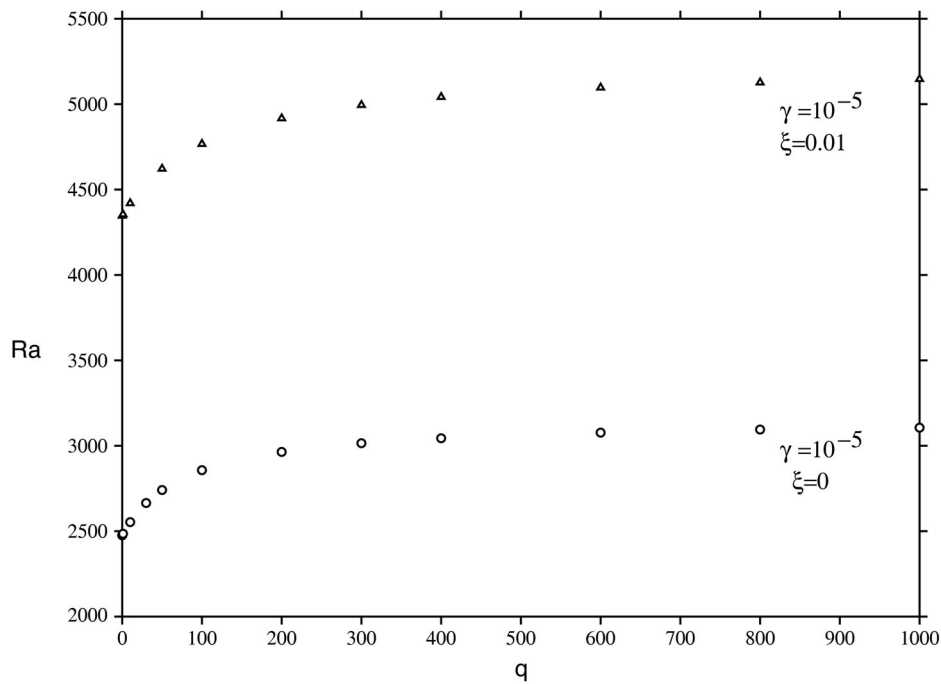
FIGURE 3 | Graph of Ra versus q, case III boundary conditions, general adherence. $\gamma = 10^{-5}, \xi = 0.01, \gamma = 10^{-5}$, and $\xi = 0$.
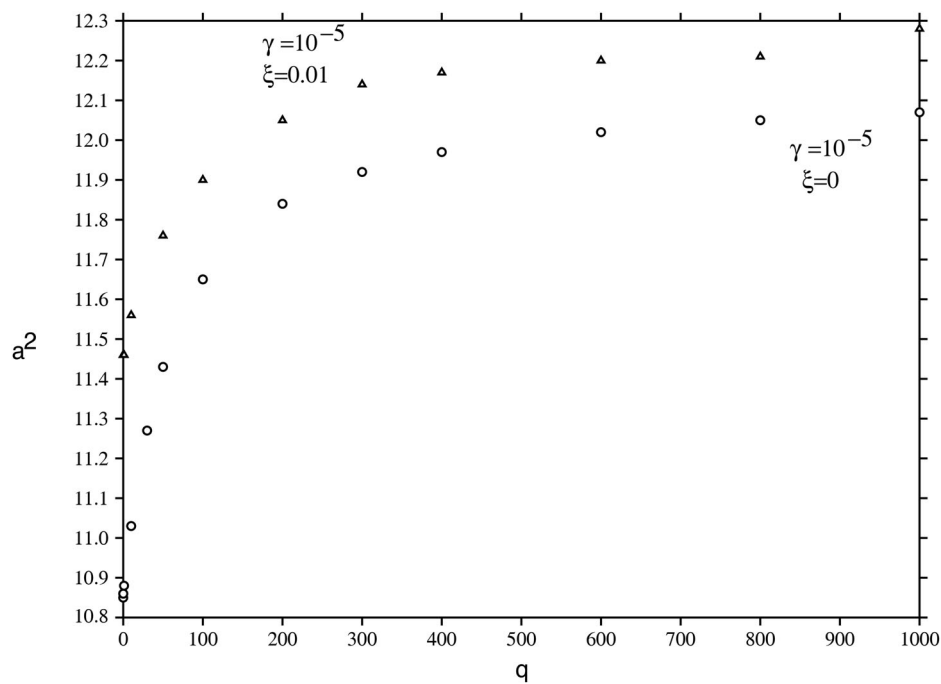

FIGURE 4 | Graph of a^2 versus q, case III boundary conditions, general adherence. $\gamma = 10^{-5}, \xi = 0.01, \gamma = 10^{-5}$, and $\xi = 0$.

The study of thermal convection for higher-order fluids can be very interesting from the technological viewpoint: for instance, in [47] it is described a novel method in energy production, where a convective motion in a bath of suitable fluid induces the creation of electricity via the pyroelectric effect with a PZT ceramic plate of thickness several μm (see for more details [47, 67]). A careful control of the convective motion is necessary in a small bath and we believe a fluid with long molecules could be employed to ensure accuracy. Such a fluid will need to be modeled by higher spatial gradients.

Furthermore, recent applications of solar pond technology have incorporated phase-change materials and other additives into the saline water to enhance electricity production efficiency (see [68–70]). The complexity of the resulting fluid can be more accurately modeled with a higher-order Navier–Stokes theory. This approach, which predicts the onset of

Studies in Applied Mathematics, 2025

TABLE 3 | Critical Rayleigh and wave numbers for boundary conditions of Case III, general adherence, versus q. The first two columns with Ra, a^2 are for $\gamma = 10^{-5}, \xi = 0$, whereas the second two columns with Ra, a^2 are for $\gamma = 10^{-5}, \xi = 0.01$.

Ra	a^2	Ra	a^2	q
2476.26	10.85	4346.97	11.47	0
2484.86	10.88	4354.86	11.47	1
2553.37	11.03	4420.06	11.56	10
2857.04	11.65	4766.95	11.90	100
3105.80	12.07	5147	12.28	1000
3155.21	12.13	5236.80	12.28	∞

convective instability at a significantly higher Rayleigh number, could prove beneficial in advancing the effectiveness of this technology. Moreover, it has been realized recently that the efficiency of a solar pond may be greatly increased by using a mixture of coal and cinder at the base ([71–74]). Such a porous medium will have a double porosity structure and in the micropores we believe a higher gradient theory for an incompressible fluid will be required for accurate assessment. Such a porous material is known as bidisperse and convection in such is well-known [75, 76], although in the solar pond case one would need to adapt the theory of convection in a fluid layer overlying a bidisperse porous medium developed in [77].

Finally, convection in nanofluids is a very hot topic in heat transfer and renewable energy research (see, e.g., [78]). A nanofluid is a suspension of typically metallic oxides in a carrier fluid and there is clear evidence that a nanofluid does not behave like a linearly viscous Navier–Stokes fluid (see, e.g., [79]). For example, a CuO nanofluid suspension contains particles of the shape of a prolate spheroid of aspect ratio 3 (see [79]). Such a molecular liquid is well-known to display non-Newtonian behavior (see, e.g. [1]), where a flattened velocity profile is observed in Poiseuille flow instead of the parabolic one of Navier–Stokes theory. Such behavior in fluid suspensions has been known for many years, see [80], and a higher-order velocity gradient theory does not suffer from the drawback of a parabolic profile. Hence, a [28] sixth-order theory is likely to also be suited to a proper description of convection in a nanofluid suspension.

Conflicts of Interest

The authors declare no conflicts of interest.

Data Availability Statement

Data sharing not applicable to this article as no data sets were generated or analyzed during the current study.

References

1. K. P. Travis, B. D. Todd, and D. J. Evans, "Poiseuille Flow of Molecular Liquids," *Physica A: Statistical Mechanics and Its Applications* 240 (1997): 315–327.

2. K. P. Travis, B. D. Todd, and D. J. Evans, "Departure From Navier-Stokes Hydrodynamics in Confined Liquids," *Physical Review E* 55, no. 4 (1997): 4288–4295, https://link.aps.org/doi/10.1103/PhysRevE.55.4288.

3. V. K. Kalantarov and E. S. Titi, "Global Attractors and Determining Modes for the 3D Navier-Stokes-Voigt Equations," *Chinese Annals of Mathematics, Series B* 30 (2009): 697–714.

4. V. K. Kalantarov and E. S. Titi, "Global Stabilization of the Navier-Stokes-Voigt and the Damped Nonlinear Wave Equations by a Finite Number of Feedback Controllers," *Discrete and Continuous Dynamical Systems - Series B* 23 (2018): 1325–1345.

5. A. O. Celebi, V. K. Kalantarov, and M. Polat, "Global Attractors for 2D Navier-Stokes-Voigt Equations in an Unbounded Domain," *Applicable Analysis* 88 (2009): 381–392.

6. P. D. Damázio, P. Manholi, and A. L. Silvestre, "L^q Theory of the Kelvin-Voigt Equations in Bounded Domains," *Journal of Differential Equations* 260 (2016): 8242–8260.

7. V. K. Kalantarov, B. Levant, and E. S. Titi, "Gevrey Regularity of the Global Attractor of the 3D Navier-Stokes-Voigt Equations," *Journal of Nonlinear Science* 19 (2009): 133–152.

8. T. Sukacheva, "Solvability of a Nonstationary Thermal Convection Problem for a Viscoelastic Compressible Fluid," *Partial Differential Equations* 36 (2000): 1225–1232.

9. T. Sukacheva, "Oskolov Models and Sobolev Type Equations," *Bulletin of South Ural State Technical University, Series: Mathematical Modelling and Programming* 15 (2022): 5–22.

10. A. P. Oskolkov, "Initial-Boundary Value Problems for the Equations of Kelvin-Voigt Fluids and Oldroyd Fluids," *Proceedings of the Steklov Institute of Mathematics* 179 (1988): 126–164.

11. A. P. Oskolkov, "Nonlocal Problems for the Equations of Motion of Kelvin-Voigt Fluids," *Journal of Mathematical Sciences* 75 (1995): 2058–2078.

12. A. P. Oskolkov and R. Shadiev, "Towards a Theory of Global Solvability on $[0, \infty)$ of Initial-Boundary Value Problems for the Equations of Motion of Oldroyd and Kelvin-Voigt Fluids," *Journal of Mathematical Sciences* 68 (1994): 240–253.

13. G. A. Sviridyuk and T. G. Sukacheva, "On the Solvability of a Nonstationary Problem Describing the Dynamics of an Incompressible Viscoelastic Fluid," *Mathematical Notes* 63 (1998): 388–395.

14. T. G. Sukacheva and O. P. Matveeva, "On a Homogeneous Model of the Non-Compressible Viscoelastic Kelvin-Voigt Fluid of the Non-Zero Order," *Journal of Samara State Technical University, Series: Physical and Mathematical Sciences* 5 (2010): 33–41.

15. T. G. Sukacheva and A. O. Kondyukov, "On a Class of Sobolev Type Equations," *Bulletin of South Ural State Technical University, Series: Mathematical Modelling and Programming* 7 (2014): 5–21.

16. B. Straughan, "Thermosolutal Convection With a Navier-Stokes-Voigt Fluid," *Applied Mathematics and Optimization* 83 (2021): 2587–2599.

17. B. Straughan, "Competitive Double Diffusive Convection in a Kelvin-Voigt Fluid of Order One," *Applied Mathematics and Optimization* 84 (2021): 631–650.

18. O. A. Ladyzhenskaya, "New Equations for the Description of Motions of Viscous Incompressible Fluids and Global Solvability of Their Boundary Value Problems," *Trudy Matematicheskogo Instituta imeni V.A. Steklova* 102 (1967): 85–104.

19. O. A. Ladyzhenskaya, "Attractors for Modifications of the Three-Dimensional Navier-Stokes Equations," *Philosophical Transactions of the Royal Society A* 99 (2000): 173–190.

20. V. V. Zhikov, "Solvability of Generalized Navier-Stokes Equations," *Doklady Mathematics* 78 (2006): 896–900.

21. B. Straughan, "Sharp Global Nonlinear Stability for Temperature-Dependent Viscosity Convection," *Proceedings of the Royal Society A* 458 (2002): 1773–1782.

22. I. C. Christov, "Soft Hydraulics: From Newtonian to Complex Fluid Flows Through Compliant Conduits," *Journal of Physics: Condensed Matter* 34 (2022): 063001.

23. X. Wang and I. C. Christov, "Theory of Flow Induced Deformation of Shallow Compliant Microchannels With Thick Walls," *Proceedings of the Royal Society A* 475 (2019): 20190513.

24. X. Wang, S. D. Pande, and I. C. Christov, "Flow Rate-Pressure Drop Relations for New Configurations of Slender Compliant Tubes Arising in Microfluidics," *Mechanics Research Communications* 126 (2022): 104016.

25. V. Anand, J. D. J. Rathinaraj, and I. C. Christov, "Non-Newtonian Fluid Structure Interactions: Static Response of a Microchannel due to Internal Flow of a Power Law Fluid," *Journal of Non-Newtonian Fluid Mechanics* 264 (2019): 62–72.

26. V. Anand and I. C. Christov, "Revisiting Steady Viscous Flow of a Generalised Newtonian Fluid Through a Slender Elastic Tube Using Shell Theory," *Zeitschrift für Angewandte Mathematik und Mechanik* 101 (2021): e201900309.

27. E. Fried and M. E. Gurtin, "Tractions, Balances, and Boundary Conditions for Nonsimple Materials With Application to Flow at Small Length Scales," *Archive for Rational Mechanics and Analysis* 182 (2006): 513–554.

28. A. Musesti, "Isotropic Linear Constitutive Relations for Nonsimple Fluids," *Acta Mechanica* 204 (2009): 81–88.

29. M. Degiovanni, A. Marzocchi, and S. Mastaglio, "Existence, Uniqueness and Regularity for the Second-Gradient Navier-Stokes Equations in Exterior Domains," in *Waves in Flows*, ed. T. Bodnár, G. P. Galdi, and Š. Necasová (Birkhüuser, 2021), 181–202.

30. G. G. Giusteri, A. Marzocchi, and A. Musesti, "Nonsimple Isotropic Incompressible Linear Fluids Surrounding One-Dimensional Structures," *Acta Mechanica* 217 (2011): 191–204.

31. M. Degiovanni, A. Marzocchi, and A. Musesti, "Edge-Force Densities and Second-Order Powers," *Annali di Matematica Pura ed Applicata* 185 (2006): 81–103.

32. V. Nikolaevskiy, "Dynamics of Viscoelastic Media With Internal Oscillators," in *Recent Advances in Engineering Science*, Lecture Notes in Engineering, Vol. 39 (Springer, 1989), 210–221.

33. I. Beresnev and V. Nikolaevskiy, "A Model for Nonlinear Seismic Waves in a Medium With Instability," *Physica D: Nonlinear Phenomena* 66, no. 1 (1993): 1–6, https://www.sciencedirect.com/science/article/pii/016727899390217O.

34. S. M. Cox and P. C. Matthews, "Pattern Formation in the Damped Nikolaevskiy Equation," *Physical Review E* 76 (2007): 056202, https://link.aps.org/doi/10.1103/PhysRevE.76.056202.

35. M. I. Tribelsky, "Patterns in Dissipative Systems With Weakly Broken Continuous Symmetry," *Physical Review E* 77 (2008): 035202, https://link.aps.org/doi/10.1103/PhysRevE.77.035202.

36. G. Panasenko and R. Stavre, "Asymptotic Analysis of a Periodic Flow in a Thin Channel With Visco-Elastic Wall," *Journal de Mathématiques Pures et Appliquées* 85, no. 4 (2006): 558–579, https://www.sciencedirect.com/science/article/pii/S0021782405001236.

37. M. Bukal and B. Muha, "A Review on Rigorous Derivation of Reduced Models for Fluid-Structure Interaction Systems," in *Waves in Flows*, ed. T. Bodnár, G. P. Galdi, and Š. Necasová (Birkhäuser, 2021), 203–237.

38. A. Barletta, "The Boussinesq Approximation for Buoyant Flows," *Mechanics Research Communications* 124 (2022): 103939.

39. D. A. S. Rees and A. Barletta, "When Does the Onset of Convection in an Inclined Porous Layer Become Subcritical?" *Mechanics Research Communications* 125 (2022): 103992.

40. D. A. S. Rees and L. Storesletten, "The Onset of Convection in a Two-Layered Porous Medium With Anisotropic Permeability," *Transport in Porous Media* 128 (2019): 345–362.

41. C. C. Wang and F. Chen, "The Bimodal Instability of Thermal Convection in a Tall Vertical Annulus," *Physics of Fluids* 34 (2022): 104102.

42. C. C. Wang and F. Chen, "On the Double-Diffusive Layer Formation in the Vertical Annulus Driven by Radial Thermal and Salinity Gradients," *Mechanics Research Communications* 100 (2022): 103991, https://doi.org/10.1016/j.mechrescom.2022.103991.

43. G. Arnone and F. Capone, "Density Inversion Phenomena in Porous Penetrative Convection," *International Journal of Non-Linear Mechanics* 147 (2022): 104198.

44. F. Capone, R. De Luca, and M. Gentile, "Coriolis Effect on Thermal Convection in a Rotating Bidispersive Porous Layer," *Proceedings of the Royal Society A* 476 (2020): 20190875.

45. F. Capone and G. Massa, "The Effects of Vadasz Term, Anisotropy and Rotation on Bidisperse Convection," *International Journal of Non-Linear Mechanics* 135 (2021): 103749.

46. F. Capone and J. A. Gianfrani, "Natural Convection in a Fluid Saturating an Anisotropic Porous Medium in LTNE: Effect of Depth-Dependent Viscosity," *Acta Mechanica* 233 (2022): 4535–4548.

47. F. Zahara El Fatnani, F. Guyomar, D. Belhora, M. Mazroui, Y. Boughaleb, and A. Hajjaji, "A New Concept to Harvest Thermal Energy Using Pyroelectric Effect and Rayleigh-Bénard Convections," *European Physical Journal Plus* 131, no. 8 (2016): 252.

48. P. Germain, "La Méthode des Puissances Virtuelles en Mécanique des Milieux Continus. Première Partie. Théorie du Second Gradient," *Journal de Mécanique* 12 (1973): 235–274.

49. P. Germain, "The Method of Virtual Power in Continuum Mechanics. Part 2: Microstructure," *SIAM Journal on Applied Mathematics* 25, no. 3 (1973): 556–575, http://www.jstor.org/stable/2100123.

50. J. Slomka and J. Dunkel, "Generalized Navier-Stokes Equations for Active Suspensions," *European Physical Journal Special Topics* 224 (2015): 1349–1358.

51. D. A. S. Rees and A. Mojtabi, "The Effect of Conducting Boundaries on Weakly Nonlinear Darcy-Bénard Convection," *Transport in Porous Media* 88 (2011): 45–63.

52. A. Barletta and D. A. S. Rees, "Local Thermal Non-Equilibrium Effects in the Darcy-Bénard Instability With Isoflux Boundary Conditions," *International Journal of Heat and Mass Transfer* 55 (2012): 384–394.

53. D. A. S. Rees and A. Mojtabi, "The Effect of Conducting Boundaries on Lapwood-Prats Convection," *International Journal of Heat and Mass Transfer* 65 (2013): 765–778.

54. A. Barletta, P. A. Tyvand, and H. S. Nygard, "Onset of Thermal Convection in a Porous Layer With Mixed Boundary Conditions," *Journal of Engineering Mathematics* 91 (2015): 105–120.

55. D. A. Nield and A. V. Kuznetsov, "Do Isoflux Boundary Conditions Inhibit Oscillatory Double-Diffusive Convection?" *Transport in Porous Media* 112 (2016): 609–618.

56. A. V. Mohammad and D. A. S. Rees, "The Effect of Conducting Boundaries on the Onset of Convection in a Porous Layer Heated From Below by Inclined Heating," *Transport in Porous Media* 117 (2017): 189–206.

57. A. Barletta and M. Celli, "The Horton-Rogers-Lapwood Problem for an Inclined Porous Layer With Permeable Boundaries," *Proceedings of the Royal Society A* 474 (2018): 20180021.

58. S. Chandrasekhar, *Hydrodynamic and Hydromagnetic Stability* (Dover, 1981).

59. B. Spain, *Tensor Calculus* (Oliver and Boyd, 1953).

60. G. P. Galdi and B. Straughan, "Exchange of Stabilities, Symmetry, and Nonlinear Stability," *Archive for Rational Mechanics and Analysis* 89 (1985): 211–228.

61. G. Giantesio, A. Girelli, C. Lonati, A. Marzocchi, A. Musesti, and B. Straughan, "Thermal Convection in a Higher Velocity Gradient and Higher Temperature Gradient Fluid," *Journal of Mathematical Fluid Mechanics* 27, no. 3 (2025): 47.

62. J. J. Dongarra, B. Straughan, and D. W. Walker, "Chebyshev Tau-QZ Algorithm Methods for Calculating Spectra of Hydrodynamic Stability Problems," *Applied Numerical Mathematics* 22 (1996): 399–435.

63. C. B. Moler and G. W. Stewart, *An Algorithm for the Generalized Matrix Eigenvalue Problem $Ax = \lambda Bx$*, University of Texas at Austin, Technical Report, 1971.

64. A. E. Green, P. M. Naghdi, and R. S. Rivlin, "Directors and Multipolar Displacements in Continuum Mechanics," *International Journal of Engineering Science* 2 (1965): 611–620.

65. A. E. Green and R. S. Rivlin, "Multipolar Continuum Mechanics," *Archive for Rational Mechanics and Analysis* 17 (1964): 113–147.

66. A. E. Green and R. S. Rivlin, "The Relation Between Director and Multipolar Theories in Continuum Mechanics," *Zeitschrift für Angewandte Mathematik und Physik* 18 (1967): 208–218.

67. F. Z. El Fatnani, M. Mazroui, and D. Guyomar, "Optimization of Pyroelectric Conversion of Thermal Energy Through the PZT Ceramic Buzzer and Natural Convection," *European Physical Journal Plus* 133 (2018): 1–10.

68. A. A. Abdullah, K. A. Lindsay, and A. F. AbdelGawad, "Parsimonious Constitutive Expressions with Good Accuracy and Suitable for Modelling the Properties of Aqueous Sodium Chloride in Solar Ponds," *Solar Energy* 122 (2015): 617–629.

69. I. Mahfoudh, P. Principi, R. Fioretti, and M. Safi, "Experimental Studies on the Effect of Using Phase Change Materials in a Salinity-Gradient Solar Pond Under a Solar Simulator," *Solar Energy* 186 (2019): 335–346.

70. J. Yu, Q. Wu, L. Bu, et al., "Experimental Study on Improving Lithium Extraction Efficiency of Salinity-Gradient Solar Pond Through Sodium Carbonate Addition and Agitation," *Solar Energy* 242 (2022): 364–377.

71. H. Wang, L. G. Zhang, and Y. Y. Mei, "Investigation on the Exergy Performance of Salt Gradient Solar Ponds with Porous Media," *International Journal of Exergy* 25, no. 1 (2018): 34–53.

72. H. Wang, Q. Wu, Y. Mei, L. Zhang, and S. Pang, "A Study on Exergetic Performance of Using Porous Media in the Salt Gradient Solar Pond," *Applied Thermal Engineering* 136 (2018): 301–308.

73. P. Dineshkumar and M. Raja, "An Experimental Study on Trapezoidal Salt Gradient Solar Pond Using Magnesium Sulfate ($MgSO_4$) Salt and Coal Cinder," *Journal of Thermal Analysis and Calorimetry* 147, no. 19 (2022): 10525–10532.

74. G. Yan, B. Teng, D. H. Elkamchouchi, et al., "Analysis of Portable Solar Concrete Ponds by Using Coal Cinder to Trap Thermal Energy of Sustainable Building Using Artificial Intelligence," *Fuel* 348 (2023): 128253.

75. B. Straughan, "Anisotropic Bidispersive Convection," *Proceedings of the Royal Society A* 475, no. 2227 (2019): 20190206.

76. M. Gentile and B. Straughan, "Bidispersive Thermal Convection With Relatively Large Macropores," *Journal of Fluid Mechanics* 898 (2020): A14.

77. P. Dondl and B. Straughan, "Thermal Convection in a Linearly Viscous Fluid Overlying a Bidisperse Porous Medium," *Studies in Applied Mathematics* 154, no. 1 (2025): e12799.

78. M. H. Chang and A. C. Ruo, "Rayleigh-Bénard Instability in Nanofluids: Effect of Gravity Settling," *Journal of Fluid Mechanics* 950 (2022): A37.

79. K. Kwak and C. Kim, "Viscosity and Thermal Conductivity of Copper Oxide Nanofluid Dispersed in Ethylene Glycol," *Korea-Australia Rheology Journal* 17 (2005): 35–40.

80. H. Fröhlich and R. Sack, "Theory of Rheological Properties of Dispersions," *Proceedings of the Royal Society A* 185 (1946): 415–430.